ACS Medicinal Chemistry Letters

Letter

Cite This: ACS Med. Chem. Lett. 2018, 9, 685−690

Structure−Activity Relationship of Novel and Selective Biaryl-Chroman GPR40 AgoPAMs

Helen Y. Chen,*[,†] Christopher W. Plummer,[†] Dong Xiao,[†] Harry R. Chobanian,[†,§] Duane DeMong,[†] Michael Miller,[†] Maria E. Trujillo,[∥] Melissa Kirkland,[∥] Daniel Kosinski,[∥] Joel Mane,[∥] Michele Pachanski,[∥] Boonlert Cheewatrakoolpong,[∥] Jerry Di Salvo,[⊥] Brande Thomas-Fowlkes,[⊥] Sarah Souza,[⊥] Daniel A. Tatosian,[§] Qing Chen,[§] Michael J. Hafey,[§] Robert Houle,[§] Andrew F. Nolting,[‡] Robert Orr,[‡] Juliann Ehrhart,[∥] Adam B. Weinglass,[⊥] Richard Tschirret-Guth,[§] Andrew D. Howard,[∥] and Steven L. Colletti[†]

[†]Departments of Discovery Chemistry, [‡]Process Chemistry, [§]Pharmacokinetics, Pharmacodynamics and Drug Metabolism, [∥]In Vivo Pharmacology, and [⊥]In Vitro Pharmacology, Merck & Co., Inc., Kenilworth, New Jersey 07033, United States

Supporting Information

ABSTRACT: A series of biaryl chromans exhibiting potent and selective agonism for the GPR40 receptor with positive allosteric modulation of endogenous ligands (AgoPAM) were discovered as potential therapeutics for the treatment of type II diabetes. Optimization of physicochemical properties through modification of the pendant aryl rings resulted in the identification of compound *AP5*, which possesses an improved metabolic profile while demonstrating sustained glucose lowering.

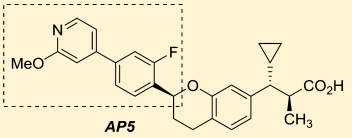

KEYWORDS: *GPR40, FFA1, GPCR, diabetes, insulin secretagogue, AgoPAM, chroman*

The GPR40 (FFAR1 or FFA1) receptor has recently attracted much interest as a novel target for the treatment of type 2 diabetes due to its ability to stimulate insulin secretion upon activation by fatty acids, in a glucose-dependent fashion.[1−3] GPR40 agonists are theorized to reduce the risk of hypoglycemia as compared to other insulin secretagogues.[4−7] Thus far, all of the GPR40 agonists that have been assessed in a clinical setting have been pharmacologically classified as partial agonists. However, researchers at Amgen[8−10] and Bristol-Myers-Squibb[11] have recently disclosed several GPR40 agonists that exhibit superior levels of receptor activation and *in vivo* efficacy, by operating as full agonists with positive allosteric modulation (AgoPAMs)[12,13] of endogenous ligands such as docosahexaenoic acid (DHA). In addition to directly stimulating more insulin secretion via the pancreas, they drive GLP-1 secretion in the gut, potentially accounting for the observed enhancement in preclinical efficacy over partial agonists.[14]

We recently reported the discovery of a novel class of biaryl chromans (***1*** and ***2***) that operate as selective GPR40 AgoPAMs.[15] Although these compounds demonstrated superior *in vivo* glucose lowering efficacy over GPR40 partial agonists such as TAK-875 with no indication of desensitization in rat 2-week and 4-week studies,[16] these initial analogs possessed the potential to form phenol metabolites and were potent inhibitors of the bile salt export pump (BSEP).[17,18] Herein, we report how these issues were addressed through a systematic exploration of the pendant aryl A and B rings (Figure 1) leading to the discovery of ***AP5***, a metabolically more stable GPR40 AgoPAM.

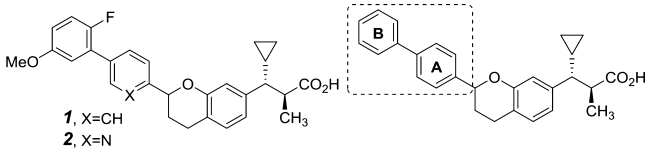

Figure 1. GPR40 AgoPAM structural leads.

Scheme 1. Library Synthesis for B-Ring Modifications[a]

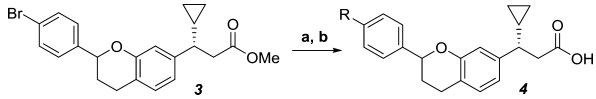

[a]Reagents and conditions: (a) R-B(OH)$_2$, 2 M K_2CO_3, Pd(dtbpf)Cl_2, dioxane, 90 °C, 3 h; (b) 1 N NaOH, MeOH, rt, 3 h (8−44% yield over 2 steps).

Our SAR investigation of the aryl B-ring began with a library synthesis based on the model system ***4*** and culminated in the discovery of key substitutions critical for potency (Table 1). Suzuki coupling of the intermediate ***3***[19] with the appropriately substituted aryl boronic acids followed by saponification afforded the desired chromans as a mixture of diastereomers (Scheme 1).

Initially, compounds were tested as diastereomeric mixtures in a cell-based assay, which measures inositol monophosphate (IP1) accumulation in a recombinant hGPR40/HEK293 cell

Received: March 29, 2018
Accepted: June 11, 2018
Published: June 14, 2018

DOI: 10.1021/acsmedchemlett.8b00149
ACS Med. Chem. Lett. 2018, 9, 685−690

Table 1. Exploration of B-Ring SAR

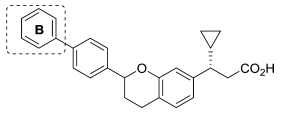

B-Ring	Cpd	hIP1 EC_{50}[a] (nM) 0% HS[b] ± SD (%act)	+100% HS ± SD (%act)	clogD (pH 7.4)[c] / PSA[d]
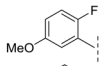	*5*	7 ± 4.7 (359%)	1227 ± 325 (188%)	4.07 / 56
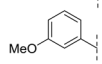	*6*	23 ± 5.6 (394%)	4033 ± 2327 (223%)	3.49 / 56
	*7*	133 ± 26 (452%)	5442 ± 2596 (57%)	3.72 / 47
	*8*	391 ± 150 (422%)	4580 ± 1795 (231%)	2.97 / 67
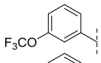	*9*	934 ± 285 (385%)	6431 ± 2124 (73%)	4.52 / 56
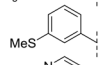	*10*	165 ± 46 (500%)	5174 (144%)	4.29 / 47
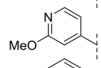	*11*	19 ± 5.6 (401%)	2561 ± 476 (229%)	2.78 / 69
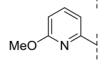	*12*	304 ± 115 (535%)	>10000 (2.4%)	2.82 / 69
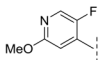	*13*	11 ± 2.9 (460%)	1206 ± 95 (224%)	3.35 / 69

[a]Mean of at least 2 runs. [b]HS = human serum. [c]Calculated cLogD at pH 7.4 using ACD Percepta software. [d]Calculated polar surface area using the TPSA method published in J. Med. Chem. 2000, 43, 3714-3717.

line designed to differentiate the efficacy of full and partial agonists as described in Plummer et al. (2017).[15,20] In addition, this assay was performed in the presence of 100% human serum (HS) to assess the impact of plasma protein on potency (EC_{50}).

We began our investigation by determining the impact of the *meta*-methoxy and *ortho*-fluoro substituents present in our lead compounds ***1*** and ***2*** on *in vitro* potency. Compound ***5***[15] is listed in Table 1 for reference. Removing the fluorine substituent in the *ortho* position as in ***6*** led to a 3−4-fold loss in potency. Next, in an effort to remove the metabolic liability of the methoxy group, we sought to remove it altogether as in ***7*** or replace it with other substituents such as a thioether (***10***) or a trifluoromethyl group (***9***). These modifications were less tolerated and resulted in a substantial loss in functional potency. The corresponding phenol analog ***8*** was also shown to be less active. Efforts to further improve physicochemical properties and thereby mitigate potential liabilites for phenol metabolites arising from cleavage of the methoxy group led us to incorporate heteroatoms into the B-ring as in compounds ***11***−***13***. Although the introduction of the pyridyl B-ring did increase PSA and reduce cLogD values, it became clear that the placement of the nitrogen atom was critical for potency. The nitrogen in the *para*-position proved to be optimal as demonstrated by the 16-fold improvement in IP1 potency of ***11*** over its *ortho*-regioisomer ***12***. Interestingly with the pyridyl B-ring, the impact of the ortho-fluorine substituent on potency was less pronouced, resulting in compounds ***11*** and ***13*** being essentially equipotent. In particular, compound ***13*** had a comparable IP1 potency and serum shift profile to the reference compound ***5***.

With the optimal B-ring substitutions identified, we focused our attention on combining B-ring modifications with A-ring

Table 2. A and B-Ring SAR in the α-Methyl Series

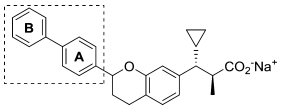

	Cpd	hIP1 EC_{50}[a] (nM) 0% ± SD / 100% ± SD HS[b,c]	ipGTT[d] (3 mg/kg)	hplc logD[e] / PSA
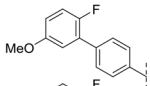	*14*	1.1 ± 0.44 / 146 ± 58	-103%	2.94 / 56
	15	2.6 ± 1.1 / 127 ± 66	-102%	
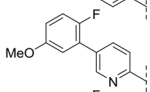	*16*	1.7 ± 1.2 / 1379 ± 636	-99%	2.25 / 69
	17	3.1 ± 1.5 / 247 ± 148	-100%	
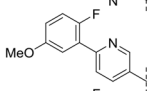	*18*	24 ± 5.6 / 5332 ± 1280	--	2.29 / 69
	19	13 ± 1.6 / 2468 ± 1822	--	
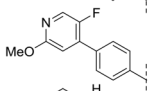	*20*	0.9 ± 0.66 / 66 ± 9.4	-59%	2.68 / 69
	21	<0.2 / 105 ± 37	-88%	
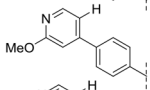	*22*	1.6 ± 0.31 / 382 ± 82	-49%	2.30 / 69
	23	5.9 ± 1.2 / 521 ± 50	-7%	
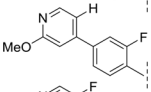	*AP5*	0.8 ± 0.16 / 35 ± 16	-103%	2.51 / 69
	25	8.2 ± 4.0 / 920 ± 412	-84%	
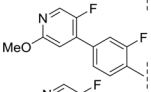	*26*	<0.2 / 36 ± 0.79	-72%	2.97 / 69
	27	1.2 ± 0.17 / 328 ± 44	-38%	
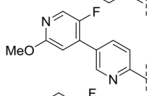	*28*	<0.2 / 1031 ± 228	-102%	1.98 / 82
	29	2.7 ± 1.7 / 243 ± 163	-108%	
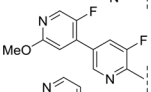	*30*	6.8 ± 0.80 / 382 ± 30	--	2.36 / 82
	31	1.6 ± 0.22 / 757 ± 47	--	
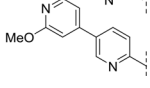	*32*	1.9 ± 0.11 / 838 ± 85	--	1.74 / 82
	33	4.4 ± 0.98 / 462 ± 17	--	

[a]Mean of at least two runs. [b]HS = human serum. [c]% Activation >179%[22]. [d]% Inhibition of net glucose AUC. [e]Experimentally determined; see Supporting Information.

Scheme 2. Achiral Synthesis of *28* and *29* Using HDA[a]

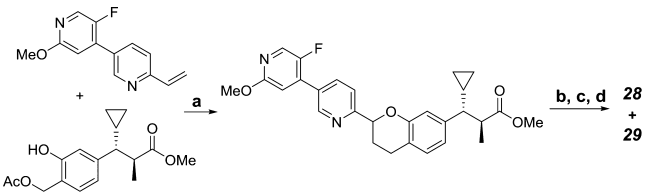

[a]Reagents and conditions: (a) xylenes, 170 °C, 50 min, 41%; (b) 1 M aqueous LiOH, MeOH/THF, 65 °C, 19 h, 89%; (c) SFC separation: Chiral-pak AD-H (50 × 250 mm; 65% MeOH/CO_2, 67%; (d) 1 M aqueous NaOH, MeCN/H_2O, 95%.

exploration in the more active alpha-methyl series (Table 2, compounds ***14***−***33***). As previously reported, installation of a methyl group alpha to the carboxylic acid in the *S*-configuration (*trans*-relative configuration) not only afforded a remarkable improvement in potency but also reduced the magnitude of the plasma protein shift on potency.[15]

Compounds were initially tested in both the human (hGPR40/HEK293) and rat (rGPR40/CHO-K1) cell lines for IP1 accumulation.[20] In general, rat IP1 EC_{50} values were consistent with human IP1 EC_{50} values and are given for select compounds listed in Table 4.[21] Compounds that demonstrated an hIP1 EC_{50} < 20 nM against the GPR40 receptor (% activation >200%)[22] and selectivity over the GPR120 receptor

DOI: 10.1021/acsmedchemlett.8b00149
ACS Med. Chem. Lett. 2018, 9, 685−690

Scheme 3. Stereoselective Synthesis of *AP5*[a]

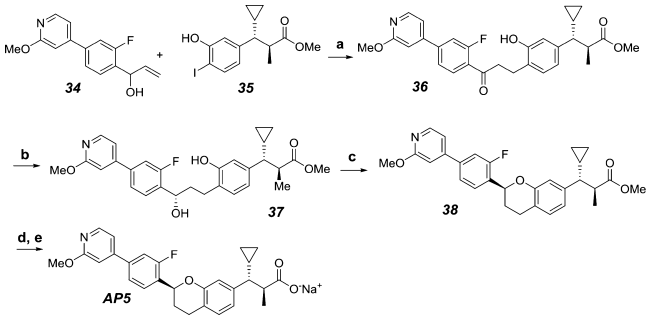

[a]Reagents and conditions: (a) *t*-BuX-Phos Palladacycle, Cy_2NMe, toluene, 90 °C, 18 h, 49%; (b) formic acid, NEt_3, RuCl[(*R*,*R*)-Tsdpen](Mesitylene), EtOAc, 22 h, quant.; (c) tBu_3P, DIAD, THF, 1 h, 94%; purity upgrade by SFC, 74%; (d) 1 M aqueous LiOH, MeOH/THF, 55−58 °C, 17 h, 96%; (e) 1 M aqueous NaOH, MeCN/H_2O, 95%.

Table 3. PK Comparison of Key Compounds

		Wistar-Han Rat PK[a]			
Cpd	f_u	Cl (mL/min/kg)	V_{dss} (L/kg)	$T_{1/2}$ (h)	F (%)
14	0.005	3.1	0.41	3.5	50
16	0.003	1.1	0.35	6.2	50
AP5	0.0002	2.8	0.48	3.7	81
29	0.001	1.2	0.41	6.4	100

[a]Administered at a dose of 1 mg/kg iv, 2 mg/kg po.

Table 4. Rat IP1, GK Rat oGTT, BSEP, and Off-Target Activity Comparison of Key Compounds

Cmpd	rat IP1[a] (EC_{50} nm ± SD)	GK rat oGTT MED[b] (pl conc[c] @ 3 h, dose)	Off-target Hits[d] #	BSEP[e] (IC_{50} μM ± SEM)
14	1.2 ± 0.35	3.0 μm @ 10 mg/kg	9	1.4 ± 0.1
16	2.3 ± 0.40	13.9 μm @ 30 mg/kg	3	0.3 ± 0.04
AP5	**0.49 ± 0.28**	**4.9 μm @ 10 mg/kg**	**4**	**3.5 ± 0.2**
29	5.2 ± 1.6	32 μm @ 30 mg/kg	1	3.2 ± 0.4

[a]Mean of at least two runs, % activation >370%.[22] [b]MED = maximum efficacious dose. [c]pl conc = plasma concentration. [d]>50% inhibition @ 10 μM; see Supporting Information for specific receptors. [e]Mean of three measurements.

(EC_{50} > 10 uM) were then further profiled in our key *in vivo* rodent models, the rat intraperitoneal glucose tolerance test (ipGTT),[23] and the Goto Kakizaki rat oral glucose tolerance test (oGTT).[24] The rat ipGTT was used to screen compounds for *in vivo* efficacy at a fixed dose of 3 mg/kg, and the percent inhibition of blood glucose AUC compared to control is reported (Table 2). Further prioritization of active compounds was accomplished by dose titration in the Goto Kakizaki rat oGTT, where glucose lowering was examined across a range of doses (0.1 mg/kg−30 mg/kg). The dose and plasma concentrations at the three hour time point that afforded maximum efficacious glucose lowering (MED) are represented in Table 4.

Utilizing the hetero-Diels−Alder (HDA) methodology described in our early work,[15,19] we were able to quickly prepare compounds listed in Table 2, varying substituents and heteroatoms in both the A and B rings in a modular fashion (Scheme 2). In general, electron-rich dienophiles delivered better yields in the HDA reaction. Although the mixture of

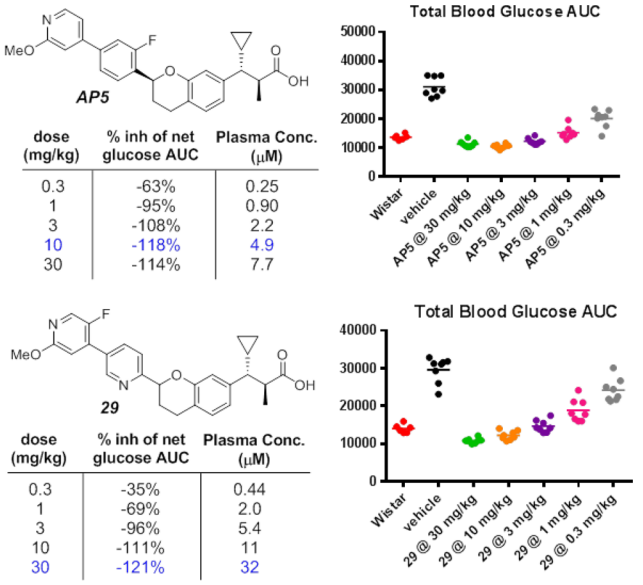

Figure 2. GK rat oGTT titrations for ***AP5*** and ***29***.

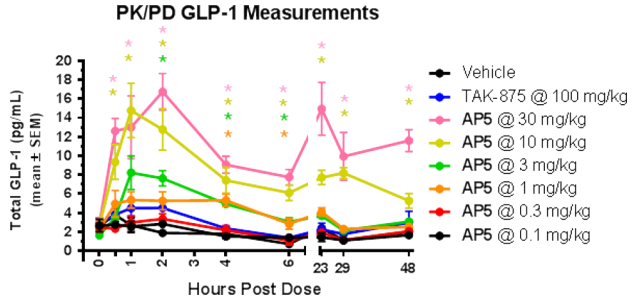

Figure 3. Dose-dependent GLP-1 secretion[31] with ***AP5***.

diastereomers was readily separable by SFC, the absolute configuration of the chroman ring was not determined.

The diastereomeric pairs, ***14/15*** and ***16/17***, described in our earlier work,[15] are listed in Table 2 for comparison. Consistent with previous observations, applying the (*S*)-*α* methyl phenyl propionic acid headpiece to the analogs (***5***, ***11***, and ***13***) containing the optimal B-ring modifications attenuated serum shift by 100-fold and increased potency in the hIP1 assay (diastereomeric pairs ***14/15***, ***20/21***, and ***22/23***). In general, the chroman stereochemistry had minimal effect on *in vitro* potency, with both diastereomers being active, and further differentiation was only observed in the magnitude of their serum-shifted IP1 potency. For example, in the case of the diastereomic pair, ***28*** and ***29***, the impact of human serum on IP1 potency was far greater for ***28*** (>5000-fold shift) compared to ***29*** (170-fold shift).

In an effort to further reduce logD and increase PSA, we replaced the A-ring phenyl with a pyridine ring. As observed with the B-ring SAR, the location of the heteroatom was critical for activity. By moving the nitrogen atom in the *ortho*-position relative to the chroman ring (***16/17***), a 10-fold improvement in hIP1 potency compared to the *meta*-position (***18/19***) was observed. Further improvement in potency and *in vivo* efficacy was achieved through the installation of a fluorine atom on either the A or B ring. Diastereomeric pairs ***AP5/25*** and ***20/21*** demonstrated better potency and glucose lowering than the nonfluorinated compounds ***22/23***. However, simultaneously installing fluorine in both the A and B ring

DOI: 10.1021/acsmedchemlett.8b00149
ACS Med. Chem. Lett. 2018, 9, 685−690

Table 5. PK Profile of *AP5* in Preclinical Species[a]

Species	f_u	Cl_{int}, hep (mL/min/kg)	Cl_p (mL/min/kg)	V_{dss} (L/kg)	$T_{1/2}$, eff (h)	F (%)
Rat	0.00021	241	2.8	0.48	3.7	81
Dog	0.015	126	1.6	0.45	6.9	79
Rhesus	0.00071	102	0.72	0.48	10.0	64
Human	0.00044	111	0.58−0.98	0.45	5.3−9.0	70

[a]Administered at a dose of 1 mg/kg iv, 2 mg/kg po. [b]Human p*K* prediction based on allometry method.[29]

Table 6. Subchronic 4-Day High Dose Safety and Tolerability Study with *AP5* in Wistar Rats[a]

Dose (mg/kg/day)	$AUC_{0-24\ h}$ (μM·h)	C_{max} (μM)	C_{min} (μM)	T_{max} (h)	Body Weight Gain[b]
200	2309 ± 804	223 ± 34	70	1−2	72% decrease
750	7354 ± 2321	545 ± 81	328	1−2	90% decrease

[a]Vehicle = 0.5% (w/v) methylcellulose in deionized water. [b]Compared to concurrent controls.

did not correspond to an additive effect on ipGTT efficacy (***26***/***27*** vs ***AP5***/***25***) despite similar hIP1 potencies.

Based on the *in vitro* IP1 potency, moderate serum shift, and *in vivo* efficacy demonstrated in the ipGTT, ***AP5*** and ***29*** were selected for further profiling. A stereoselective route (Scheme 3) featuring a Noyori reduction of the ketone intermediate ***36*** to establish the chroman stereocenter[25] was utilized for the large scale preparation of ***AP5***. Ketone ***36*** was prepared via a Pd-mediated Heck coupling of the allylic alcohol ***34*** and the iodophenol ***35***. Using RuCl[(*R*,*R*)-Tsdpen](Mesitylene) catalyst, the key benzylic alcohol intermediate ***37*** was obtained as a 86:14 mixture of diastereomers enriched in the preferred "*S*" configuration. Further diastereomeric upgrade to >99% dr was accomplished with chiral SFC separation after a subsequent Mitsunobu reaction to form the chroman intermediate ***38***. Hydrolysis with aqueous LiOH and conversion to the corresponding sodium salt with aqueous NaOH afforded the final compound ***AP5***. The absolute configuration at the chroman stereocenter of ***AP5*** was further confirmed by electronic circular dichroism (ECD) of its corresponding methyl ester ***38***.[26]

The Wistar-Han rat PK profiles of ***AP5*** and ***29*** are listed in Table 3 along with ***14*** and ***16*** for comparison. Both compounds exhibited acceptable half-lives and exposures projecting to QD dosing in humans and plasma exposures ripe for further evaluation in rodents.

In the GK rat oGTT, oral administration of ***AP5*** and ***29*** 1 h before an oral dextrose challenge showed that both compounds significantly reduced blood glucose levels compared to the vehicle (Figure 2, Table 4). Compound ***AP5*** was determined to be more efficacious in this model, demonstrating maximally efficacious glucose lowering at a plasma concentration of 4.9 μM at 10 mg/kg. Compounds ***AP5*** and ***29*** were further evaluated *in vitro* for inhibition of the BSEP and found to have marginal improvement over our initial analogs, ***14*** and ***16*** (Table 4).[27] These compounds were also screened against 40 receptors that included a broad panel of GPCR's, ion channels, transporters, and enzymes at 10 μM (Table 4). The number of off-target hits with greater than 50% inhibition was reduced from nine in ***14*** to just four in ***AP5***.[28] Incorporating nitrogen atoms in both the A and B ring, as in ***29***, further reduced the number of off-target hits to one, demonstrating an excellent correlation between physical properties and off-target activity.

In addition, ***AP5*** showed enhanced GLP-1 secretion that was dose-dependent (Figure 3), consistent with the observed GPR40 AgoPAM mechanism of action.[16] In contrast, measurable GLP-1 release is not observed with partial agonists such as TAK-875.

Furthermore, ***AP5***'s acceptable rat PK profile translated into higher species including dog and monkey with a projected human oral bioavailability of 70% (Table 5). Using allometric scaling[29] from the rat, dog (beagle), and rhesus, ***AP5*** is projected to have a human dose of 7−15 mg along with a human half-life of 10−16 h making the compound suitable for QD dosing. In addition, *in vitro* metabolism studies in human hepatocytes showed that formation of phenol metabolites was not observed in ***AP5*** through the introduction of the B-ring heteroatom, with the major metabolite being formation of the acyl-gluoronide (75%).[30] In contrast, the starting analog, ***14***, showed that the B-ring phenol and its sulfonated derivative accounted for 67% of metabolites formed *in vitro* in human hepatocytes.[30]

In view of compound ***AP5***'s significant glucose lowering effect in the GK rat oGTT, demonstrated increase in GLP-1 secretion, and improved off-target and PK profile over ***14***, ***AP5*** was selected to undergo further assessment in a subchronic 4-day high dose safety and tolerability study in Wistar rats dosed at 200 and 750 mg/kg/day. Compound ***AP5***'s plasma concentration levels reached 2309 μM·h and 7354 μM·h, respectively. At these exposures, no mortalities, serum biochemistry changes (including cardiac troponin I), liver weight increases, gross findings, or changes in the functional observational battery were observed. The only observed effect was a decrease in body weight gain reported in Table 6.

In conclusion, through a systematic exploration of A and B ring SAR, ***AP5*** was identified as a potent and selective GPR40 AgoPAM that demonstrates excellent *in vivo* efficacy with a projected human dose of 7−15 mg. By introducing key modifications, such as nitrogen atom incorporation into the B ring and fluorine substitution in the A-ring, phenol metabolite formation was mitigated, off-target activity was reduced, and marginal lowering was seen in BSEP inhibition, all of which led to a clean safety and tolerability profile of ***AP5*** in a sub chronic 4-day high dose study.

■ ASSOCIATED CONTENT

Supporting Information

The Supporting Information is available free of charge on the ACS Publications website at DOI: 10.1021/acsmedchemlett.8b00149.

Experimental procedures, analytical data, assay protocols, and metabolism data. (PDF)

DOI: 10.1021/acsmedchemlett.8b00149
ACS Med. Chem. Lett. 2018, 9, 685−690

AUTHOR INFORMATION

Corresponding Author

*E-mail: helen_chen@merck.com.

ORCID

Helen Y. Chen: 0000-0002-1212-943X

Christopher W. Plummer: 0000-0001-5522-1933

Notes

The authors declare no competing financial interest.

ACKNOWLEDGMENTS

The authors would like to thank Leo Joyce, Ed Sherer, and Joe Shpungin for the structural determination of compound **38** by ECD analysis, Scott Borges for SFC Separations, Qi Gao for NMR analysis, and Rong-Sheng Yang for HRMS support.

ABBREVIATIONS

GPR40, g-protein-coupled receptor 40; GPCR, g-protein coupled receptors; FFAR1, free fatty acid receptor 1; AgoPAM, agonist-allosteric modulator; DHA, docosahexaenoic acid; GLP-1, glucagon-like peptide 1; BSEP, bile salt export pump; SAR, structure−activity relationship; h1P1, human inositol monophosphate; HS, human serum; act., activation; SD, standard deviation; SEM, standard error of mean; PSA, polar surface area; oGTT, oral glucose tolerance test; ipGTT, intraperitoneal glucose tolerance test; MED, maximum efficacious dose; PK, pharmacokinetics; HAD, Hetero-Diels−Alder; HEK293, human embryonic kidney (cell line); CHO-K1, Chinese Hamster Ovary-K1 (cell line); SFC, supercritical fluid chromatography; THF, tetrahydrofuran; ACN, acetonitrile; HPLC, high performance liquid chromatography; AUC, area under curve; dr, diastereomeric ratio; dtbpf, di-(*tert*-butylphosphino)ferrocene; DIAD, diisopropylazodicarboxylate; *t*-BuXphos Palladacycle, [2-(di-*tert*-butylphosphino)-2′,4′,6′-triisopropyl-1,1′-biphenyl][2-(2-aminoethyl)phenyl]-palladium(II) chloride; Cy_2NMe, *N*,*N*-dicyclohexylmethylamine.

REFERENCES

(1) Defronzo, R. A. From the triumvirate to the ominous octet: a new paradigm for the treatment of type II diabetes. *Diabetes* **2009**, *58*, 773−795.

(2) Itoh, Y.; Kawamata, Y.; Harada, M.; Kobayashi, M.; Fujii, R.; Fukusumi, S.; Ogi, K.; Hosoya, M.; Tanaka, Y.; Uejima, H.; Tanaka, H.; Maruyama, M.; Satah, R.; Okubo, S.; Kizawa, H.; Komatsu, H.; Matsumura, F.; Moguchi, Y.; Shinohara, T.; Hinuma, S.; Fujisawa, Y.; Fujino, M. Free fatty acids regulate insulin secretion from pancreatic β cells through GPR40. *Nature* **2003**, *422*, 173−176.

(3) Stoddart, L. A.; Smith, N. J.; Milligan, G. International union of pharmacology. LXXI. Free fatty acid receptors FFA1, −2, and −3: pharmacology and pathophysiological functions. *Pharmacol. Rev.* **2008**, *60*, 405−417.

(4) Negoro, N.; Sasaki, S.; Mikami, S.; Ito, M.; Suzuki, M.; Tsujihata, Y.; Ito, R.; Harada, A.; Takeuchi, K.; Suzuki, N.; Miyazaki, J.; Santou, T.; Odani, T.; Kanzaki, N.; Funami, M.; Tanaka, T.; Kogame, A.; Matsunaga, S.; Yasuma, T.; Momose, Y. Discovery of TAK-875: A potent, selective, and orally bioavailable GPR40 agonist. *ACS Med. Chem. Lett.* **2010**, *1*, 290−294.

(5) Christiansen, E.; Due-Hansen, M. E.; Urban, C.; Merten, N.; Pfleiderer, M.; Karlsen, K. K.; Rasmussen, S. S.; Steensgaard, M.; Hamacher, A.; Schmidt, J.; Drewke, C.; Petersen, R. K.; Kristiansen, K.; Ullrich, S.; Kostenis, E.; Kassack, M. U.; Ulven, T. Structure activity study of dihydrocinnamic acids and the discovery of the potent FFA1 (GPR40) agonist TUG-469. *ACS Med. Chem. Lett.* **2010**, *1*, 345−349.

(6) Houze, J. B.; Zhu, L.; Akerman, M.; Qiu, W.; Zhang, A. J.; Sharma, R.; Schmidt, M.; Wang, Y.; Liu, J.; Medina, J. C.; Regan, J. D.; Luo, J.; Tonn, G.; Zhang, J.; Lu, J. Y-L.; Chen, M.; Lopez, E.; Nguyen, K.; Yang, L.; Tang, L.; Tian, H.; Shuttleworth, S. J.; Lin, D. C-H. AMG-837: A potent, orally bioavailable GPR40 agonist. *Bioorg. Med. Chem. Lett.* **2012**, *22*, 1267−1270.

(7) Ge, M.; Yang, L.; Zhou, C.; Lin, S.; Tang, H.; Cline, E. D.; Malkani, S. Preparation of bicyclic compounds as antidiabetics. (2006) WO 2006083781 A1.

(8) Brown, S. P.; Dransfield, P. J.; Vimolratana, M.; Jiao, X.-Y.; Zhu, L.; Pattaropong, V.; Sun, Y.; Liu, J.; Luo, J.; Zhang, J.; Wong, S.; Zhuang, R.; Guo, Q.; Li, F.; Medina, J. C.; Swaminath, G.; Lin, D. C-H.; Houze, J. B. Discovery of AM-1638: A Potent and Orally Bioavailable GPR40/FFA1 Full Agonist. *ACS Med. Chem. Lett.* **2012**, *3*, 726−730.

(9) Wang, Y.; Liu, J.; Dransfield, P. J.; Zhu, L.; Wang, Z.; Du, X.; Jiao, X.; Su, Y.; Li, A.-R.; Brown, S. P.; Kasparian, A.; Vimolratana, M.; Yu, M.; Pattaropong, V.; Houze, J. B.; Swaminath, G.; Tran, T.; Nguyen, K.; Guo, Q.; Zhang, J.; Zhuang, R.; Li, F.; Miao, L.; Bartberger, M. D.; Correll, T. L.; Chow, D.; Wong, S.; Luo, J.; Lin, D. C-H.; Medina, J. C. Discovery and optimization of potent GPR40 full agonists containing tricyclic spirocycles. *ACS Med. Chem. Lett.* **2013**, *4*, 551−555.

(10) Du, X.; Dransfield, P. J.; Lin, D. C-H.; Wong, S.; Wang, Y.; Wang, Z.; Kohn, T.; Yu, M.; Brown, S. P.; Vimolratana, M.; Zhu, L.; Li, A.-R.; Su, Y.; Jiao, X.; Liu, J.; Swaminath, G.; Tran, T.; Luo, J.; Zhuang, R.; Zhang, J.; Guo, Q.; Li, F.; Connors, R.; Medina, J. C.; Houze, J. B. Improving the pharmacokinetics of GPR40/FFA1 full agonists. *ACS Med. Chem. Lett.* **2014**, *5*, 384−389.

(11) Ellsworth, B. A.; Shi, J.; Jurica, E. A.; Nielsen, L. L.; Wu, X.; Hernandez, A. H.; Wang, Z.; Gu, Z.; Williams, K. N.; Chen, B.; Cherney, E. C.; Ye, X.; Wang, Y.; Zhou, M.; Cao, G.; Xie, C.; Wilkes, J. J.; Liu, H.; Kunselman, L. K.; Gupta, A. K.; Jayarama, R.; Ramar, T.; Rao, J. P.; Zinker, B. A.; Sun, Q.; Dierks, E. A.; Foster, K. A.; Wang, T.; Cvijic, M. E.; Whaley, J. M.; Robl, J. A.; Ewing, W. R. Discovery of BMS-986118, a dual MOA GPR40 agonist that produces glucose-dependent insulin and GLP-1 secretion. *248th ACS National Meeting*, San Francisco, CA, United States,, August 10−14, 2014.

(12) For a review of GPCR allostery, see: Wootten, D.; Christopoulos, A.; Sexton, P. M. Emerging paradigms in GPCR allostery: implications for drug discovery. *Nat. Rev. Drug Discovery* **2013**, *12* (8), 630−644.

(13) For precedent of agoPAMs applied to other GPCRs, see: Noetzel, M. J.; Rook, J. M.; Vinson, P. N.; Cho, H. P.; Days, E.; Zhou, Y.; Rodriguez, A. L.; Lavreysen, H.; Stauffer, S. R.; Niswender, C. M.; Xiang, Z.; Daniels, J. S.; Jones, C. K.; Lindsley, C. W.; Weaver, C. D.; Conn, P. J. Functional impact of allosteric agonist activity of selective positive allosteric modulators of metabotropic glutamate receptor subtype 5 in regulating central nervous system function. *Mol. Pharmacol.* **2012**, *81* (2), 120−133.

(14) Edfalk, S.; Steneberg, P.; Edlund, H. GPR40 is expressed in enteroendocrine cells and mediates free fatty acid stimulation of incretin secretion. *Diabetes* **2008**, *57*, 2280−2287.

(15) Plummer, C. W.; Clements, M. J.; Chen, H.; Rajagopalan, M.; Josien, H.; Hagmann, W. K.; Miller, M.; Trujillo, J. E.; Kirkland, M.; Kosinski, D.; Mane, J.; Pachanski, M.; Cheewatrakoolpong, B.; Nolting, A. F.; Orr, R.; Christensen, M.; Campeau, L. C.; Wright, M. J.; Bugianesi, R.; Souza, S.; Zhang, X.; Di Salvo, J.; Weinglass, A. B.; Tschirret-Guth, R.; Nargund, R.; Howard, A. D.; Colletti, S. L. Design and Synthesis of Novel, Selective GPR40 AgoPAMs. *ACS Med. Chem. Lett.* **2017**, *8*, 221−226.

(16) Trujillo, M. E.; Pachanski, M. J.; Kirkland, M. E.; Kosinski, D. T.; Mane, J.; Cheewatrakoolpong, B.; Xue, J.; Szeto, D.; Forrest, G.; Miller, C.; Bunzel, M.; Plummer, C. W.; Chobanian, H. R.; Miller, M. W.; Souza, S.; Thomas-Fowlkes, B. S.; Ogawa, A. M.; Weinglass, A. B.; Di Salvo, J.; Li, X.; Feng, Y.; Tatosian, D. A.; Howard, A. D.; Colletti, S. L. GPR40 partial agonists and AgoPAMs: Differentiating effects on glucose and hormonal secretions in the rodent. *PLoS One* **2017**, *12* (10), No. e0186033.

DOI: 10.1021/acsmedchemlett.8b00149
ACS Med. Chem. Lett. 2018, 9, 685−690

(17) Aleo, M. D.; Luo, Y.; Swiss, R.; Bonin, P. D.; Potter, D. M.; Will, Y. Human drug-induced liver injury severity is highly associated with dual inhibition of liver mitochondrial function and bile salt export pump. *Hepatology* **2014**, *60* (3), 1015−1022.
(18) Dawson, S.; Stahl, S.; Paul, N.; Barber, J.; Kenna, J. G. In Vitro Inhibition of the Bile Salt Export Pump Correlates with Risk of Cholestatic Drug-Induced Liver Injury in Humans. *Drug Metab. Dispos.* **2012**, *40* (1), 130−138.
(19) Brockunier, L. L.; Chen, H.; Chobanian, H. R.; Clements, M. J.; Crespo, A., Demong, D. E.; Guo, Y.; Hagmann, W. K.; Marcantonio, K. M.; Miller, M.; Pio, B.; Plummer, C. W.; Xiao, D. Antidiabetic bicyclic compounds (2014), WO2014130608 A1.
(20) See Supporting Information for *in vitro* inositol phosphate turnover (hIP1 and rIP1) study protocols.
(21) See Supporting Information for rat IP1 EC50s of compounds in Table 2 with *in vivo* ipGTT data.
(22) Comparable level of receptor activation to AM-1638 as discussed in footnote 16.
(23) See Supporting Information for *in vivo* ipGTT study protocol.
(24) See Supporting Information for *in vivo* GK rat oGTT study protocol.
(25) Orr, R. K.; Campeau, L. C.; Chobanian, H. R.; McCabe Dunn, J. M.; Pio, B.; Plummer, C. W.; Nolting, A.; Ruck, R. T. A Modular Synthesis of 2-Alkyl- and 2-Arylchromans via a Three-Step Sequence. *Synthesis* **2017**, *49* (3), 657−666.
(26) See Supporting Information for ECD determination.
(27) See Supporting Information for *in vitro* BSEP study protocol.
(28) See Supporting Information for specific receptors.
(29) Tang, H.; Hussain, A.; Leal, M.; Mayersohn, M.; Fluhler, E. Interspecies Prediction of Human Drug Clearance Based on Scaling Data from One or Two Animal Species. *Drug Metab. Dispos.* **2007**, *35* (10), 1886−1893.
(30) See Supporting Information for metabolites of ***AP5*** and ***14***.
(31) See Supporting Information for *in vivo* GLP-1 study protocol.

DOI: 10.1021/acsmedchemlett.8b00149
ACS Med. Chem. Lett. 2018, 9, 685−690